Hindawi
International Journal of Photoenergy
Volume 2020, Article ID 9682428, 17 pages
https://doi.org/10.1155/2020/9682428

Research Article

Optimization of Energy Consumption in Net-Zero Energy Buildings with Increasing Thermal Comfort of Occupants

Mohsen Mahdavi Adeli, Said Farahat, and Faramarz Sarhaddi

Department of Mechanical Engineering, University of Sistan and Baluchestan, Zahedan, Iran

Correspondence should be addressed to Said Farahat; said.farahat.usb@gmail.com

Received 8 September 2019; Revised 23 October 2019; Accepted 14 November 2019; Published 24 January 2020

Academic Editor: Yong Chen

Residential and commercial buildings consume approximately 60% of the world's electricity. It is almost impossible to provide a general definition of thermal comfort, because the feeling of thermal comfort is affected by varying preferences and specific traits of the population living in different climate zones. Considering that no studies have been conducted on thermal satisfaction of net-zero energy buildings prior to this date, one of the objectives of the present study is to draw a comparison between the thermal parameters for evaluation of thermal comfort of a net-zero energy building occupants. In so doing, the given building for this study is first optimized for the target parameters of thermal comfort and energy consumption, and, hence, a net-zero energy building is formed. Subsequent to obtaining the acceptable thermal comfort range, the computational analyses required to determine the temperature for thermal comfort are carried out using the Computational Fluid Dynamics (CFD) model. The findings of this study demonstrate that to reach net-zero energy buildings, solar energy alone is not able to supply the energy consumption of buildings and other types of energy should also be used. Furthermore, it is observed that optimum thermal comfort is achieved in moderate seasons.

1. Introduction

Most people spend most of the time in residential buildings, factories, or administrative offices. With the rapid development of urbanization, the United Nations has predicted that by 2050, 66% of population will live in urban or suburb areas [1]. Hence, it is necessary to achieve one of the most important factors in sustainable urban life by constructing energy-efficient buildings. The construction sector is the largest producer of greenhouse gases (GHG) in the world. They are responsible for about 40% of the world's energy, 40% of nonrenewable resources, 25% of the world's water, and approximately 30% of greenhouse gas emissions [1]. The main purpose of any effort for the development of energy-efficient buildings is to provide thermal comfort with minimal energy consumption for a particular building in a particular climate. One of the most important points is to ensure that reducing energy needs does not affect thermal comfort of the residents. Air temperature is the most important variable for determining thermal comfort. However, temperature is not the only factor, and other factors affect the processes of heat exchange on the human body such as humidity, air velocity, and radiation [2]. There are basically two fundamental viewpoint on thermal comfort: (1) static viewpoint and (2) adaptive viewpoint. Static stand point defines the predicted mean vote (PMV) parameter by using the combination of a mathematical model of heat transfer and experimental relations of human comfort. This kind of viewpoint has been employed in many previous researches. But the adaptive approach is based on adaptation: if an alternation occurs in the thermal comfort conditions and the discomfort is created, somehow people will react to this condition to achieve comfort. Therefore, unlike the PMV method, the adaptive model could not be described with details and, theoretically, requires a procedure for field studies [2].

Cao et al. investigated a hybrid zero-energy system that includes a zero energy building and an H_2-fueled integrated

vehicle system under German and Finnish conditions. They concluded that optimal combination of photovoltaic (PV) and wind turbine for the net-zero energy occurs when the PV generation reaches 60% and 20% under German and Finnish climates, respectively [3].

Aryal and Leephakpreeda investigated the effect of the partitions of a building with an air conditioning system on energy consumption and thermal comfort using CFD analysis and concluded that the partition installation increased thermal comfort of residents, but also increased energy consumption by 24%. They recommended the use of CFD models to determine parameters such as infiltration [4].

Zhang et al. optimized the air temperature of the room by ventilation of air from two aspects of thermal comfort and energy saving and concluded that the air velocity in the room should be considered in calculations. Also, they obtained a 7.8% reduction in energy consumption by considering the thermal comfort for residents [5].

Lu et al. investigated thermal comfort and thermal adaptation for areas with a warm and humid climate and concluded that the temperature range would not necessarily coincide with comfort of residents. This investigation also indicated that a humid environment could not provide comfort for humans at any temperature [6].

Alfano et al. performed a thermal comfort analysis for a school building in Italy which was exposed to natural ventilation in summer and winter (with a case study of 4000 students) and concluded that Fanger's relation would be improved by applying an expectancy factor of 0.9. Expectancy factor, multiplied by the PMV, returns an improved vote that keeps into account the difference in occupant expectancy of nonventilated buildings [7].

Xu et al. investigated the energy management of a building under the PMV thermal comfort model by an uncertainty method and concluded that based on the description of thermal comfort by a PMV model, energy and cost savings and cost reductions for the demand for an electric global network were obtained. Numerical results illustrated that their method was robust due to uncertainty in error prediction and results in a reduction of more than 60% without computationally perceptible damage to system performance [8].

Fabbri evaluated the thermal comfort in a kindergarten with the PMV and PPD models by data mining and a questionnaire. He concluded that the PMV coefficient of children was higher in comparison with that of adults and suggested that the age to be considered in the PMV model [9].

Hu and Li reduced the classification of rules of thermal comfort control by employing an optimal method. They demonstrated that their proposed thermal comfort control could be used to achieve thermal comfort and reduce energy consumption and consumption costs [10].

Hwang and Shu investigated the thermal comfort of a glass-paneled building based on the PMV thermal comfort model to save energy consumption. The parametric analysis was done on glass façade with various overhang depths, glazing type, window-wall ratio (WWR), and glazing area. The results showed that both thermal comfort and energy savings were achieved even in full glass-paneled buildings with the precise design of components of glass façade [11].

Kang et al. evaluated the capabilities of energy saving in an administrative building under thermal comfort control and investigated the effect of variations of the average radiant temperature. Their results showed that the use of thermal comfort control is a more sensible way to achieve thermal comfort and save energy [12].

Kim et al. developed an adaptive PMV model to improve its predictive performance. They considered the differences between actual mean votes (AMV) of residents in a building and proposed a model that could enhance the performance of the PMV model and play an important role in reducing the consumption of the cooling energy in the building [13].

Nada et al. investigated thermal comfort, temperature distribution, and air flow pattern using CFD in a theater building, which yielded optimal performance temperature, proper temperature, and velocity of inlet air [14].

Orosa and Oliveira compared the adaptive models and PMV and proposed a new method for thermal comfort. The results indicated that the new model in this study, which considered relative humidity within space, is closer to adaptive methods than to PMV methods [15].

Pourshaghaghy and Omidvari experimented the PMV-PPD model in an old state hospital and concluded that most of the thermal comfort problems occur on winter mornings and the worst heat conditions fall at noon in the summer days, and they proposed that the insulation operations be employed for all doors and windows [16].

Volkov et al. developed a model for the thermal comfort of internal spaces of three types of social buildings (kindergarten, school, and hospital) and concluded that other parameters such as age, population sensitivity, and sickness could affect PMV and PPD [17].

Haniff et al. optimized the scheduling of an air conditioning system in a building using the multiobjective improved global particle swarm optimization. By keeping the amount of PMV in the desired range, they reduced electricity consumption by 46% [18].

Wei et al. investigated and studied the thermal conditions of a naturally ventilated residential room in the wet climate with PMV and PPD field studies and concluded that the value of PMV was between 1 and -1, but residents had thermal comfort [19].

Deng et al. simulate two buildings for the different dry and humid climates of Madrid (Spain) and warm and humid climates of Shanghai (China), and the performance of buildings and systems used in both conditions. In their simulations, two buildings were connected to the national energy grid, and the balance of production and energy consumption was reviewed annually and per 6 minutes [20].

Wu et al. examine the energy performance and initial costs of one residential net-zero energy building (NZEB) in different weather regions, using a TRNSYS model confirmed by operational data of a whole year. They reported that energy and cost data as well as the required PV capacity can make heating, ventilation, and air conditioning (HVAC) and PV designs for design and planning residential NZEBs in different climate zones [21].

More than half of consumed energy in buildings is related to HVAC and lighting systems. But different values for these conditions will be obtained by variability of different climates. This research has been performed considering the weather conditions in Zahedan, where the cooling and lighting loads of buildings are dominant consumed loads. Therefore, in order to optimize the energy consumption of the building, more emphasis has been placed on the investigation of different HVAC and lighting systems to find an optimal solution to reduce the energy consumption of the building.

The present study changed the values of the overall heat transfer coefficient for walls, types of windows and ceilings, building direction, number of summer air exchange loads, and other passive systems; these are analyzed, and the optimal mode is selected with the lowest energy consumption. After achieving a methodology, the net energy consumption of the system is obtained and discussed for energy generation. In most of the previous researches, the mentioned energy consumption has been analyzed separately. In this study, these energies are considered simultaneously. Also, unlike many previous researches, balancing electricity will also be considered zero or low energy in home energy calculations. Meanwhile, thermal comfort is considered as an objective function in the optimization problem. The purpose of the NZEB in the present study is to reach a point where power generation on site can provide all its electricity. It should be noted that the NZEB must be a realistic goal of reducing energy consumption and CO_2 emissions, not just a theoretical idea [22].

2. Methods

The use of renewable energies in a modeled building of the present research and a way of exchange of electrical energy with the network and electrical storage (battery) are indicated in Figure 1. As shown in Figure 1, the sun and wind energies are continuous inputs of electric current of the building. Notably, unlike thermal energy, electrical energy does not have a storage capability in a simple manner after generation. For this purpose, the battery is used after the generation of electricity and converted to a storable state. In this research, firstly, the generated electricity is stored by employing the power generators connected to the battery (after supply of the electrical energy of building), then, if the battery is fully charged, the excess electricity is transmitted to the global network. It may also be sometimes possible, when the high energy load is on the building, firstly, that the stored electricity is received from the battery, and the electricity is received from the global network when the battery is completely discharged.

As shown in Figure 2, the entire processes are commenced by the modeling of the building, then energy analysis is performed and then, the optimization analysis is carried out in order to design a highly efficient building. In the following steps, solar and wind energies are added to the existing energy resources of the building, and results of their impact on the building are investigated. The crucial point is that in solving the present problem, firstly, the building must be minimized in terms of internal energy consumption with suitable orientation, WWR, insulation, selecting building materials, etc. (passive design), and then, the energy production be increased by renewable energy resources (active design). Using active design alone is not a perfect solution for designing a net-zero energy building, i.e., increasing of electricity generation by renewable energy resources to a building with high energy consumption is not an appropriate strategy to reach net-zero energy building.

2.1. Building Model. A real two-storey building with administrative use in Zahedan, Iran, has been studied for modelling, which possessed a total of 149 m^2 of foundation and its occupied volume was 513 m^3. The 3D layout of this building is illustrated in Figure 3. In addition, details of the design of the modeled building are presented in Table 1.

As explained in the previous section, to provide a part or all of the consumed energy for a net-zero energy building (NZEB), the energy production in the building should be employed. The produced energy consists of two general types: electrical and thermal. However, background research has indicated that it is possible to convert these energies to one another with some coefficients for analyzing energy in a mechanical system [23]. As shown in Figure 1, two types of photovoltaic solar energy and wind energy have been used in this study to produce electrical power considering the potential climate of Zahedan city. The characteristics of the photovoltaic panel and turbines employed in this study are listed in Tables 2 and 3, respectively.

The wind turbines also require a region with high wind gradient speeds such as Zahedan city. Environmental information and thermal comfort for the various seasons (from January to December 2018) are presented in Table 4. DesignBuilder software is the graphical interface for EnergyPlus Software used in this study that accounts for weather conditions (such as wind speed, average annual sunshine, and temperature) of a particular area to energy performance analysis [24].

In order to analyze the thermal comfort through Fanger's model, environmental data such as the air temperature, mean radiant temperature, and relative velocity of wind, are presented in Figures 4–7. The monthly diagrams for dry-bulb temperature and dew-point temperature are demonstrated in Figure 4. As can be seen, the maximum wet-bulb temperature occurred in summer, and the dew-point is almost constant throughout the year. The changes in atmospheric pressure around the building throughout the year are also indicated in Figure 5. As can be seen by the blue line in this figure, the pressure changes are negligible and can be considered to be about 87586 Pa. The annual rate of humidity is also shown in Figure 6, indicating that relative humidity around the building is not very high due to the dry climate of Zahedan city throughout the year. The relative speed of the wind and its direction are also shown in Figure 7.

2.2. Total Useful Energy Consumption Analysis. The most important loads in a building are cooling and thermal loads.

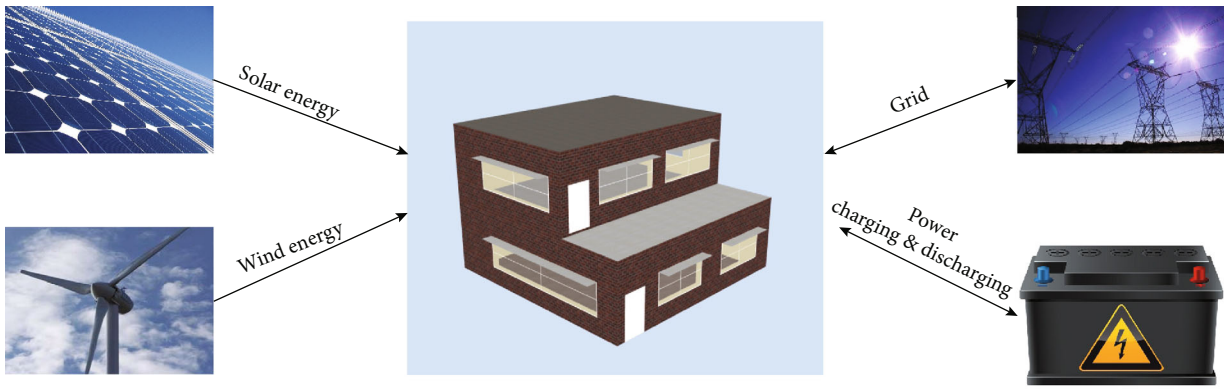

Figure 1: Energy exchange of the studied building with renewable resources, battery, and network.

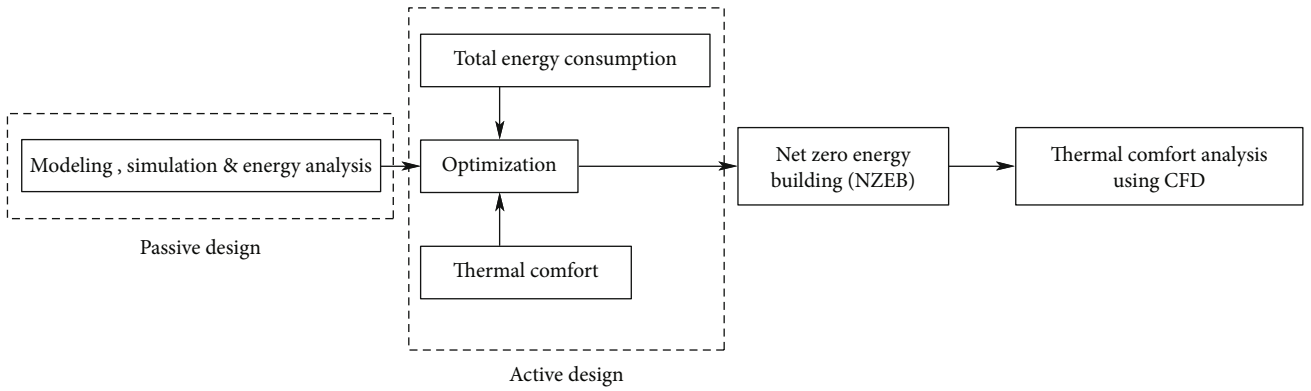

Figure 2: The analysis and problem solving strategies.

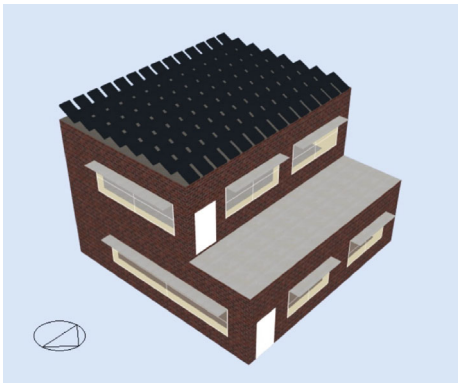

Figure 3: The modeled administrative building for analysis.

In a building, the total rate of dissipated heat and received heat must be equal, which is presented in [25]:

$$-Q_{\mathrm{HVAC}} = Q_{\mathrm{Total\ site\ energy\ consumption}} = \sum_{i=1}^{\mathrm{Nsj}} \dot{Q}_i + \sum_{i=1}^{\mathrm{Nsurface}} h_i \cdot A_i \cdot (T_{\mathrm{si}} - T_z) + \sum_{i=1}^{\mathrm{Nzones}} m_i \cdot c_p \cdot (T_{\mathrm{zi}} - T_z) + m_{\mathrm{inf}} \cdot c_p \cdot (T_{\mathrm{ext}} - T). \quad (1)$$

In the above equation, $\sum_{i=1}^{\mathrm{Nsj}} Q_i$ is the sum of the loads produced by the internal convection heat transfer, $\sum_{i=1}^{\mathrm{Nsurface}} h_i \cdot A_i \cdot (T_{\mathrm{si}} - T_z)$ is the exchanged convection heat transfer caused by the surfaces of different regions, $\sum_{i=1}^{\mathrm{Nzones}} m_i \cdot c_p \cdot (T_{\mathrm{zi}} - T_z)$ is the heat transfer resulted by the combination of air inside the regions, and $m_{\mathrm{inf}} \cdot c_p \cdot (T_{\mathrm{ext}} - T_z)$ is also the heat transfer caused by the outflow from air gaps.

Heat transfer from the building components will affect the temperatures of internal surfaces (T_{si}), and accordingly, the convection heat transfer between the building surfaces and the internal air is given in

$$-q''_{\mathrm{conv}} = q''_{\mathrm{LWX}} + q''_{\mathrm{SW}} + q''_{\mathrm{LWS}} + q''_{\mathrm{sol}} + q''_{\mathrm{ki}}, \quad (2)$$

where q''_{LWX} is the flux of the radiation heat transfer between surfaces with long wavelengths, q''_{SW} is the flux of the radiation heat transfer between lights and surfaces, and q''_{LWS} is the flux of the radiation heat transfer between surfaces and irradiators. Also, q''_{sol} is the amount of the solar radiation flux, and q''_{ki} is the amount of the conduction heat transfer from the surrounding of the building. To calculate q''_{ki}, the formula presented in Equation (3) can be used:

Table 1: Modeled building's specification and site location.

Parameters	Values/types
Program version	EnergyPlus, version 8.5.0-c87e61b44b
Hours simulated (hr)	8760
Weather file	Zahedan airport—IRN ITMY WMO#=408210
Latitude (deg)	29.48
Longitude (deg)	60.91
Elevation about sea level (m)	1378
Site orientation (deg)	0
HVAC	Ground source heat pump (GSHP), water to water heat pump, heated floor, chilled beams, nat vent
External wall U value (W/m^{2}K)	0.350
Gross wall area (m^2)	259
Internal partitions U value (W/m^{2}K)	1.639
Flat roof U value (W/m^{2}K)	0.250
Internal floor U value (W/m^{2}K)	2.929
Gross window-wall ratio (%)	19.55
Window opening area (m^2)	50.63
Glazing type	2 layers/air gap/13 mm
Window shading	0.5 m/overhang
Lighting	Compact fluorescent (CFL)
Occupancy density (people/m^2)	0.111
Operating hours (hr)	10 (8 : 00-18 : 00)
Activity of occupants	Light office work/standing/walking
Electricity density of office equipment (W/m^2)	11.77
Consumption rate of domestic hot water (DHW) (L/m^{2}day)	0.2

Table 2: Photovoltaic panel specifications.

Parameters	Values/types
Total area (m^2)	54
Fraction of surface with active PV	0.9
Efficiency (%)	15
Material	Bitumen felt
Heat transfer integration	Decoupled
Inverter efficiency (%)	90
Availability schedule	On 24/7

Table 3: Wind turbine specifications.

Parameters	Values/types
Rotor type	Horizontal-axis wind turbine
Power control	Variable-speed fixed-pitch
Overall height (m)	11
Number of blades	3
Overall wind turbine system efficiency (%)	83.5
Availability schedule	On 24/7

$$q''_{\mathrm{ki}}(t) = -Z_o T_{i,t} - \sum_{j=1}^{\mathrm{nz}} \dot{Z}_j T_{i,t-j\delta} + Y_o T_{o,t} + \sum_{j=1}^{\mathrm{nz}} Y_j T_{o,t-j\delta} + \sum_{j=1}^{\mathrm{nq}} \Psi_j q''_{\mathrm{ki},t-j\delta}, \quad (3)$$

where T is the temperature, the coefficients i and o indicate the internal and external surfaces of the building, respectively, t represents the time in one step, and Z, Y, Ψ are the internal, cross-over, and flux coefficients.

The annual rate of required energy consumed for cooling the inside of the building is also derived from Equation (4), which is in kWh/m^2·year:

$$\mathrm{CN}_{\mathrm{usf}} = \frac{1-\eta_c}{A} \times Q_{\mathrm{gn},c}, \quad (4)$$

where η_c is the loss coefficient of cooling devices, A is the total and useful coolant surface of the building, and $Q_{\mathrm{gn},c}$ is the total received flux of internal and solar heat.

As can be seen in the heating section of the building, solving these equations requires the cooling temperature to be set to certain rates in some seasons. To obtain the value of $Q_{\mathrm{gn},c}$, Equation (5) can be used:

$$Q_{\mathrm{gn},c} = Q_{\mathrm{opq}} + Q_s + Q_i, \quad (5)$$

Table 4: Site data and comfort for different months of a year.

Data/month	Jan	Feb	Mar	Apr	May	Jun	Jul	Aug	Sep	Oct	Nov	Dec
Air temp. (°C)	23.7	24.2	25.7	26.9	29.1	30.7	31.4	31.8	30.4	27.8	25.5	23.7
Radiant temp. (°C)	24.9	25.6	27.3	29.1	31.4	32.8	33.6	33.7	32.5	29.8	27.1	24.8
Operative temp.(°C)	24.3	24.6	26.5	28.0	30.2	31.7	32.5	32.8	31.5	28.8	26.3	24.3
Outside dry-bulb temp. (°C)	17.9	19.1	23.2	26.6	30.6	33.0	34.2	33.3	32.0	28.8	23.4	18.5
Outside dew-point temp. (°C)	9.4	12.0	15.5	18.2	22.3	24.2	26.7	27.2	24.6	20.8	13.5	11.8
Wind speed (m/s)	2.2	2.3	3.2	2.4	3.3	2.9	3.7	4.1	3.2	1.6	2.1	2.8
Wind direction (deg)	107.3	131.2	128.5	108.0	126.8	131.2	130.3	135.3	143.5	68.4	123.6	144.7
Solar altitude (deg)	-13.0	-8.3	-1.3	6.2	11.8	14.3	13.2	8.8	2.0	-5.5	-11.5	-14.2
Solar azimuth (deg)	189.8	190.2	191.8	193.9	194.9	194.2	193.0	193.2	194.7	195.8	194.5	191.1
Atmospheric pressure (kPa)	101.5	101.4	101.3	101.0	100.5	99.8	99.5	99.6	99.9	100.2	100.8	101.1
Direct normal solar (kWh)	108.5	104.8	135.9	114.9	119.3	163.6	123.2	139.9	117.3	106.8	95.2	95.0
Diffuse horizontal solar (kWh)	103.1	131.3	121.8	183.7	196.7	156.6	158.1	147.5	156.3	139.0	111.8	98.0

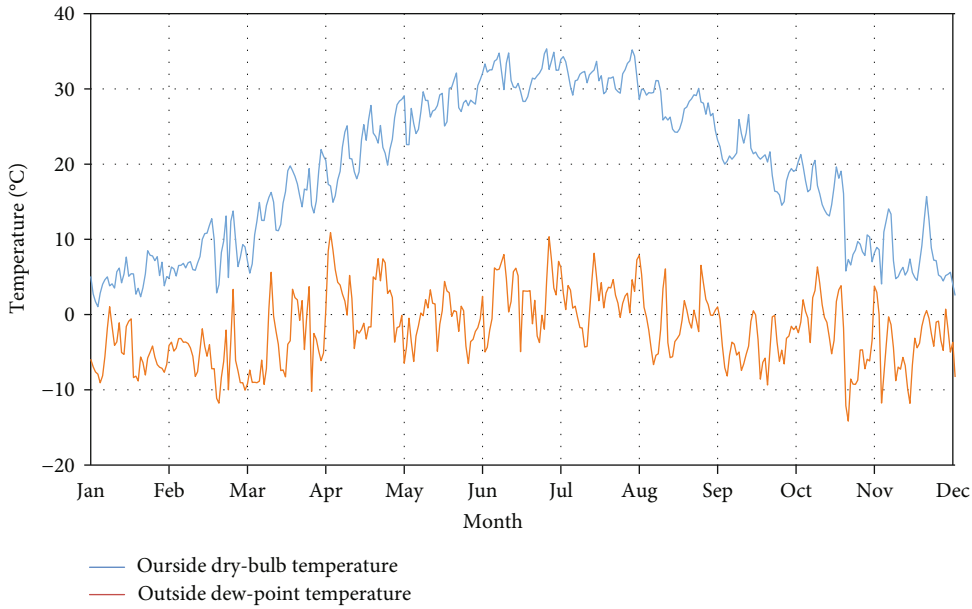

Figure 4: Monthly dry-bulb and dew-point temperature outside the building.

where Q_{opq} are internal heats caused by equipment, lights, and people living in the building, and Q_s is also the received solar heat from transparent environments (such as windows and other transparent surfaces), while Q_i is the received solar heat from opaque environments.

Finally, the heat loss from external walls (Q_{loss}) is also obtained from

$$Q_{loss} = U(T_t - T_{md}), \tag{6}$$

where U is the total heat transfer coefficient, T_t is the constant internal tem perature, and T_{md} is the daily average temperature, which are obtained from

$$T_{md} = \frac{T_{rad} + T_{air}}{2}, \tag{7}$$

where T_{rad} is the radiant temperature, and T_{air} is the air temperature.

2.3. Thermal Comfort. Thermal comfort does not seem to be a phenomenon that is defined precisely by the temperature, humidity, air flow, metabolism, etc. But these parameters should be used for mathematical modeling [26]. In the last 100 years, a lot of research has been performed on indexes and predictive models of thermal comfort as a mathematical model. The main purpose of all these models is to provide a single index that includes all relevant parameters. In this research, three of the most prominent thermal comfort

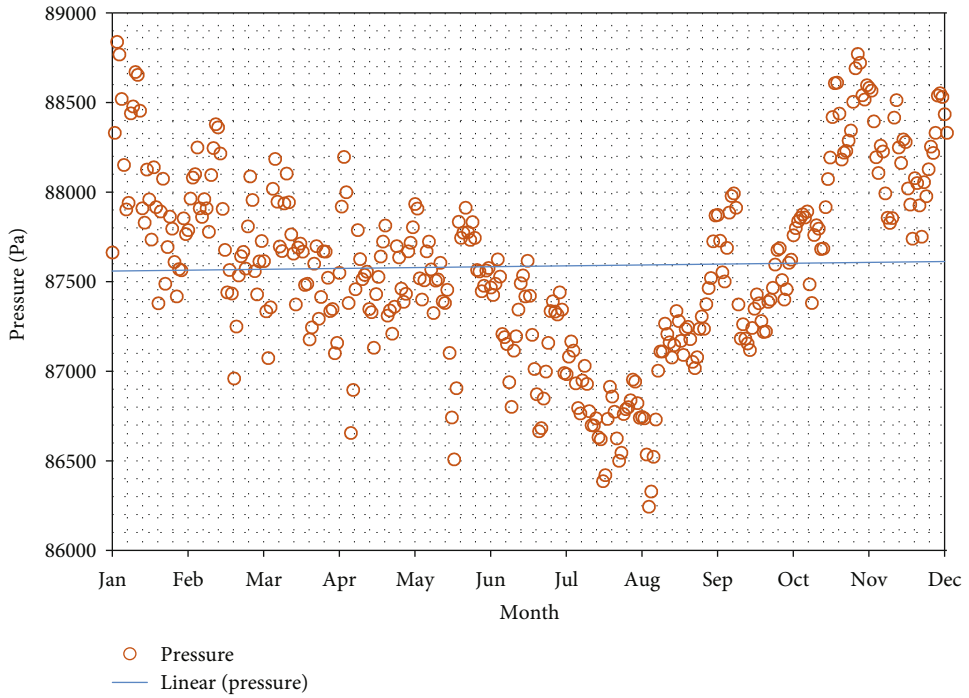

Figure 5: Monthly atmospheric pressure around the modeled building.

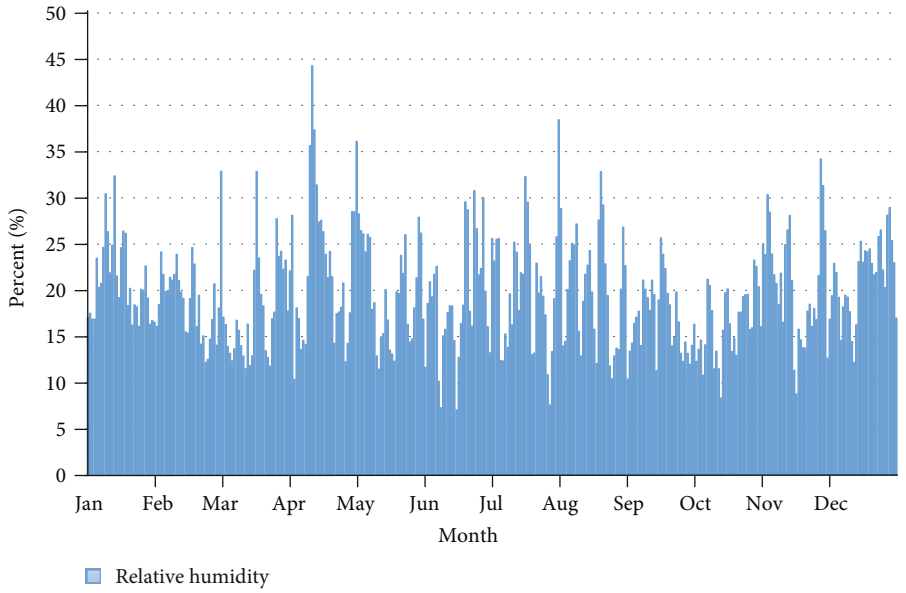

Figure 6: Annual relative humidity around the modeled building.

models have been investigated, including Fanger's Thermal Comfort Model, Pierce's Thermal Comfort Model, and the Thermal Comfort Model of the University of Kansas. All of these models are based on the concept of the first law of thermodynamics, but it seems that Fanger's Model has had the greatest impact on academic research, development of simulation software, and development of standards [2].

The equation of Fanger's Thermal Comfort to obtain the predicted mean vote (PMV) is derived from the equation of heat balance as follows [27]:

$$\begin{aligned}\mathrm{PMV} = {} & \left[0.303e^{-0.036M} + 0.028\right] \times \left\{D - 3.05 \times 10^{-3}\right. \\ & \times (5733 - 6.99D - P_v) - 0.42 \times (D - 58.15) - 1.7 \\ & \times 10^{-5} \times M \times (58.67 - P_v) - 1.4 \times 10^{-3} \times M \\ & \times (34 - T_{\mathrm{in}}) - 3.96 \times 10^{-8} \times f_{\mathrm{clo}} \times \left[(T_{\mathrm{clo}} + 273)^4\right. \\ & \left.\left. - (T_{\mathrm{mrt}} + 273)^4\right] - f_{\mathrm{clo}} \times h \times (T_{\mathrm{clo}} - T_{\mathrm{in}})\right\},\end{aligned} \tag{8}$$

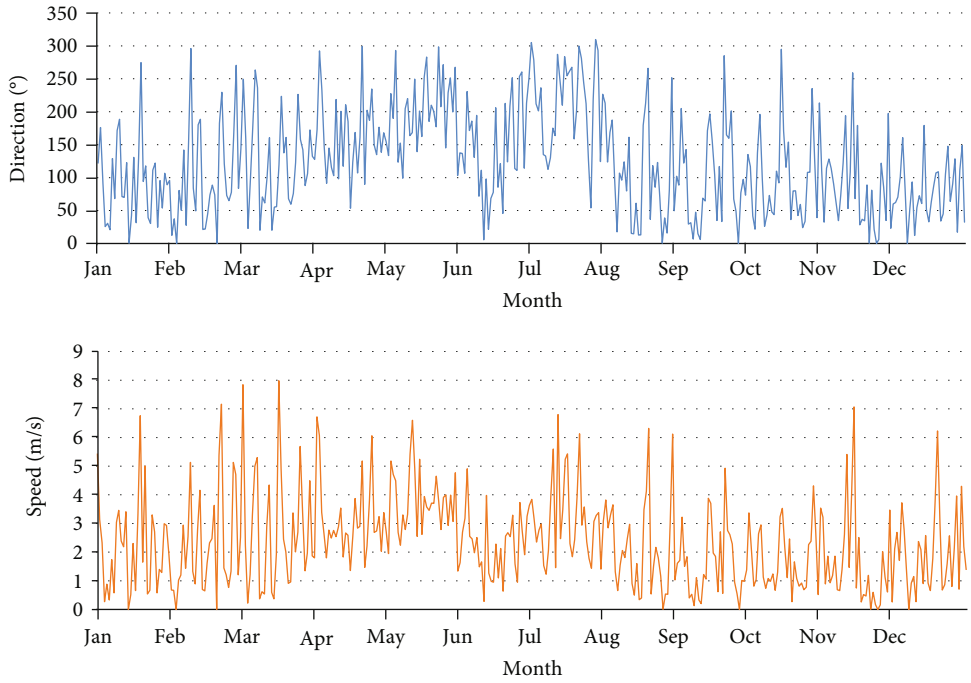

Figure 7: Relative wind speed and annual wind direction around the modeled building.

where $D = M - W$ and h is the coefficient of the convection heat transfer and is derived from

$$h = \begin{cases} 2.38 \times |T_{clo} - T_{in}|^{0.25}, & \text{if } 2.38 \times |T_{clo} - T_{in}|^{0.25} \geq 12.1 v_{rel}{}^{0.5}, \\ 12.1 \times v_{rel}{}^{0.5}, & \text{otherwise.} \end{cases} \quad (9)$$

And also for the temperature of clothes surface (T_{clo}), we have

$$T_{clo} = 35.7 - 0.028D - I_{clo} \times \left\{3.96 \times 10^{-8} \times f_{clo} \times \left[(T_{clo} + 273)^4 - (T_{mrt} + 273)^4\right] + f_{clo} \times h \times (T_{clo} - T_{in})\right\}. \quad (10)$$

And also for f_{clo} which represents the covering surface of the body with/without clothes, we have the following equation:

$$f_{clo} = \begin{cases} 1 + 1.29 \times I_{clo}, & \text{if } I_{clo} \leq 0.078 m^2 k/W, \\ 1.05 + 0.645 \times I_{clo}, & \text{otherwise,} \end{cases} \quad (11)$$

where I_{clo} is the coefficient of thermal resistance of clothes (m^2k/W). And also for the pressure of the water vapor in ambient air (P_v) in kPa, we have the following equation:

$$P_v = RH \times 610.6 \times e^{(17.26 \times T_{in})/(273.3 + T_{in})}. \quad (12)$$

In the above equations, M is the metabolic rate of the body (W/m^2), W represents the mechanical work of the body (W/m^2), and T_{clo}, T_{mrt}, and T_{in} are the surface temperature of clothes, the average radiant temperature, and the temperature of air inside the room (°C), respectively. Also, RH is relative humidity (%).

Finally, the predicted percentage of dissatisfied (PPD) can be derived from Equation (13). The relationship between PMV and PPD was seen in Figure 8.

$$PPD = 100 - 95 \times e^{-0.03353PMV^4 - 0.2179PMV^2}. \quad (13)$$

The ISO 7730: 2005 standard recommends that the appropriate PPD is approximately 10%, related to the thermal comfort range of -0.5% and +0.5% [28]. Residents inside the building are usually sitting or doing light physical activities. The metabolic rate in sitting position is $58.15 W/m^2$. Hereupon, this amount of metabolic rate has been considered in the current study. Covering is also considered as 0.6. The mechanical work of the body is also considered to be zero. The radiant mean temperature of the internal surfaces is contemplated to be equal to the outside temperature. The relative humidity according to Figure 6 is also considered to be 15% for warm and dry climates.

2.4. Optimization. The nondominated sorting genetic algorithm II (NSGA-II) is an evolutionary algorithm. Evolutionary algorithms were developed because the gradient-based and classical direct techniques have the following problems when leading with complex and nonlinear interactions [29]. Figure 9 illustrates the optimization analysis with objective functions and decision variables with the method of NSGA-II optimization. The results of this method demonstrate the most acceptable values in "Pareto Front". The red points show the Pareto Front of optimal solutions which give the

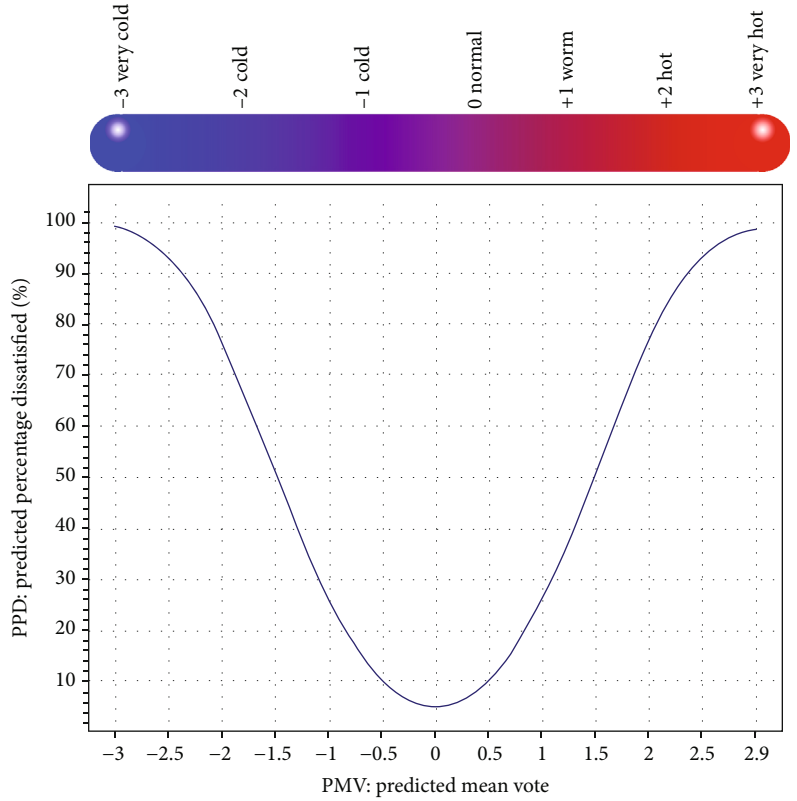

Figure 8: The relationship between PMV and PPD.

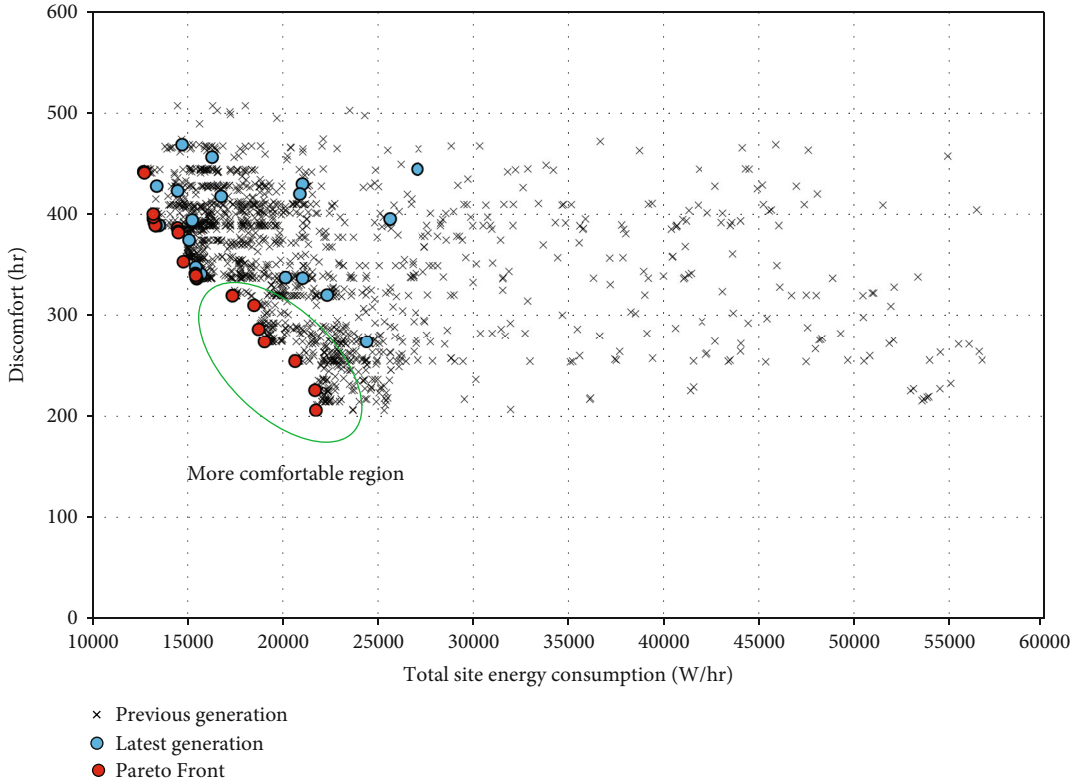

Figure 9: The optimization results and determination of Pareto Front for most optimized points.

lowest combination of discomfort hours and total site energy consumption. As can be seen in this figure, different symbols are drawn in the graph, each symbol indicating an independent design for HVAC and lighting systems. For optimizing the energy consumption of the building, three total quantities should be considered in general: thermal comfort level, total cost, and total energy consumption of building. Clearly, the comfort level should be increased, and other two quantities should be decreased to reach the objective. Obviously by using higher-efficiency systems, the energy consumption of the building is reduced, but the total cost of the building is increased. On the other hand, by increasing the comfort level of residents, there is a potential increase in the energy consumption and total costs. Therefore, it is logical to consider the level of comfort in this problem as an objective function and not a constraint. Of course, the reduction of hours of thermal comfort dissatisfaction has been considered an objective function instead of increasing thermal comfort in the present study, as shown in Figure 9.

In solving the optimization problem in the present study, about 4000 decision points have been investigated. From the obtained results, 6 points have been selected as optimal points which are shown by drawing an ellipse in Figure 9. The points close in the ellipse represent the highest level of thermal comfort of residents, considering the energy consumption of the building. The summary of these six points is given in Table 5. As seen in Table 5, the decision variables are the cooling system coefficient of performance (COP), HVAC system, Lighting, Cooling set-back temperature, and Heating set-back temperature. Also, the objective functions are Total site energy consumption (kWh) and Discomfort (hr : min).

2.5. CFD Analysis

2.5.1. Governing Equations. The governing equations of a fluid flow represent mathematical expressions of physical conservation laws. In this research, it is assumed that the air flow velocity inside the building and pressure gradients are very low. Hence, the air flow is assumed to be incompressible. The energy, momentum, and continuity equations for a 3D steady-state flow using the Cartesian Tensor signs are given in the following equations:

$$\begin{aligned}
\frac{\partial U_i}{\partial x_i} &= 0,\\
\rho U_i \frac{\partial U_i}{\partial x_i} &= -\frac{\partial P}{\partial x_j} + \frac{\partial}{\partial x_i}\left[\mu\left(\frac{\partial U_i}{\partial x_j} + \frac{\partial U_j}{\partial x_i}\right) - \rho\overline{u_i' u_j'}\right],\\
\rho c_p U_i \frac{\partial T}{\partial x_i} &= \frac{\partial}{\partial x_i}\left[\lambda\frac{\partial T}{\partial x_i} - \rho c_p \overline{u_i' T'}\right],\\
p &= \rho R T,
\end{aligned} \tag{14}$$

where T and U_i are temperature and time-mean speed, respectively. Also R, p, μ, ρ, and λ are gas constant, static pressure, viscosity, density, and thermal diffusivity, respectively. u_i', u_j', T', $\rho c_p \overline{u_i' T'}$, and $-\rho\overline{u_i' u_j'}$ are variable velocities, temperature, fluctuating heat fluxes, and Reynolds stresses, respectively.

The K-ε turbulence model is used due to its high utilization in various flow regimes and its less calculations.

2.5.2. Computational Method. In the present study, using the CFD existing in commercial version of DesignBuilder 5.0.3 software, 3D simulation of the turbulent flow inside the building has been performed using the steady-state K-ε turbulence model. The governing equations were discretized using the finite volume method. Pressure-velocity equations were coupled using the SIMPLE algorithm. The Power Law differential method is used to differentiate pressure, momentum, energy, turbulent dissipated energy, and turbulent kinetic energy equations, since this method provides better results and faster convergence in the flow and temperature distribution regions. In order to obtain exact results, it is assumed that the convergence of solution occurs when the normalized residuals of continuity, momentum, turbulence, and energy are less than 10^{-5}.

3. Results

As we know, the rate of electrical energy generated by photovoltaic panels depends on the hour, day, season, received solar radiation, and also the angle of installed photovoltaic panels. To make the simulation more real and obtain correct results, all the issues mentioned in the present study have been considered. In Figure 10, the sun position (sun path diagram) has been plotted at 11:00 AM on April 15th.

3.1. Results of Total Energy Consumption Analysis. According to Equations (1), (2), (3), (4), (5), (6), and (7), Figure 11 illustrates the results of energy analysis on the administrative building in months of a year. This figure allows to compare consumed energies, either thermal or electrical. As can be seen, some of the energies (lighting, electrical equipment, etc.) are relatively constant, and some others are variable according to the utilization of the building in seasons. For example, lighting and electrical systems (including computers and other electronic equipment) were constant throughout the year, and cooling equipment were variable, which were active only during summer.

3.2. Electrical Energy Analysis. In the analysis of electrical energy for the studied building, three different scenarios have been analyzed: the building without energy generation, the building with photovoltaic energy, and the building with photovoltaic energy and wind turbine; the characteristics of the photovoltaic panel and wind turbine are listed in Tables 2 and 3. The results are presented in Figures 12–15. In the first scenario, the diagram of consumed loads is shown as in Figure 12 (the building without electrical energy generation). It is clear that the peak energy consumption occurs during the warm seasons, mainly due to cooling loads. Figure 13 shows the total and generated consumed loads in the building with photovoltaic panels (second scenario). As can be seen in the figure, the efficiency and generation of

Table 5: Optimization of Pareto Front.

	Total site energy consumption (kWh)	Discomfort (hr : min)	Cooling system COP	HVAC	Lighting	Cooling set-back PMV (°C)	Heating set-back PMV (°C)
1	21740.3	206 : 55	4.75	VAV, air-cooled chiller, HR, outdoor air reset+mixed mode	Fluorescent, compact (CFL)	26.7	6
2	21696.9	225 : 58	4.9	VAV, air-cooled chiller, HR, outdoor air reset	Fluorescent, compact (CFL)	26.2	2.3
3	20645.7	254 : 32	5	GSHP water to water heat pump, heated floor, chilled beams, nat vent	Fluorescent, compact (CFL)	25.8	-4.6
4	19046.8	273 : 26	5	VAV, water-cooled chiller, full humidity control	T5 (16 mm diam) fluorescent, triphosphor, high-frequency control	26.7	5.4
5	18712.9	286 : 22	5	VAV, air-cooled chiller, steam humidifier, air-side HR, outdoor air reset	T5 (16 mm diam) fluorescent, triphosphor, high-frequency control	25.8	-3.9
6	18478.3	310 : 19	4.95	Fan coil unit (4 pipes) with district heating+cooling	T5 (16 mm diam) fluorescent, triphosphor, high-frequency control	25.3	6

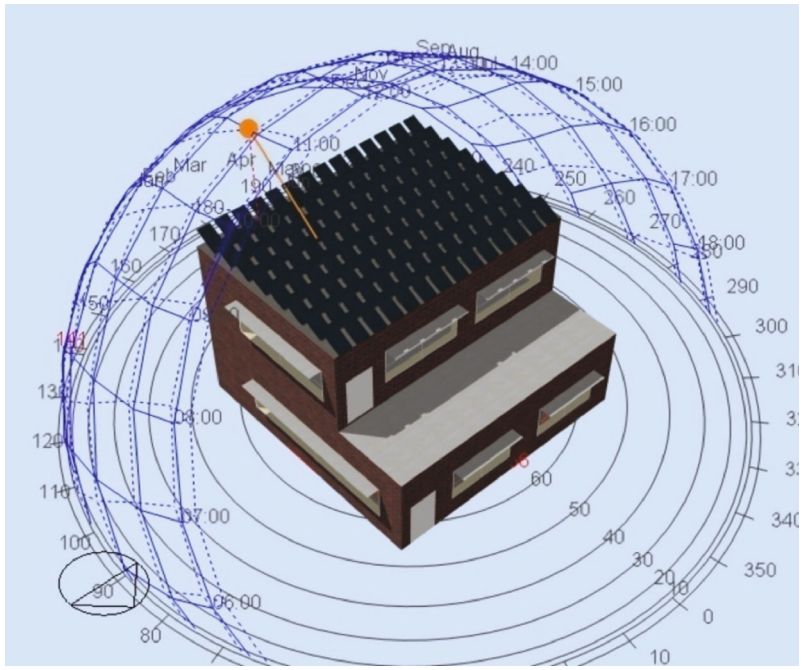

Figure 10: The schematic plan of sun radiation path in the 15th of April.

photovoltaic panels in the warm seasons of the year were higher, due to the high intensity of solar radiation. But it is clear that the energy generated by these panels is not enough already to achieve a net-zero energy building. The results show that the total annual energy received from the photovoltaic panel for this building was 13338.2 kWh. The results of electric and consumed energies for the third scenario are presented in Figure 14. As can be seen, the electrical energy generated by wind turbines was undeniably appreciated and had the capability of compensating for the lack of electricity in photovoltaic panels during the cold seasons.

The details of the monthly consumption of electric energy are shown in Figure 15 for the building in which both the photovoltaic panel and wind turbine were used (third scenario), including electrical energy used for the activity of residents and all equipment except lighting, electrical energy consumed for lighting, electrical energy consumed for cooling, and electrical energy consumed for supplying hot water. As mentioned, due to the weather condition in Zahedan city, the most energy consumed is due to the energy generated for cooling in the warm seasons, so that the maximum cooling load for this building was 1223 kWh and in July. Annual rates

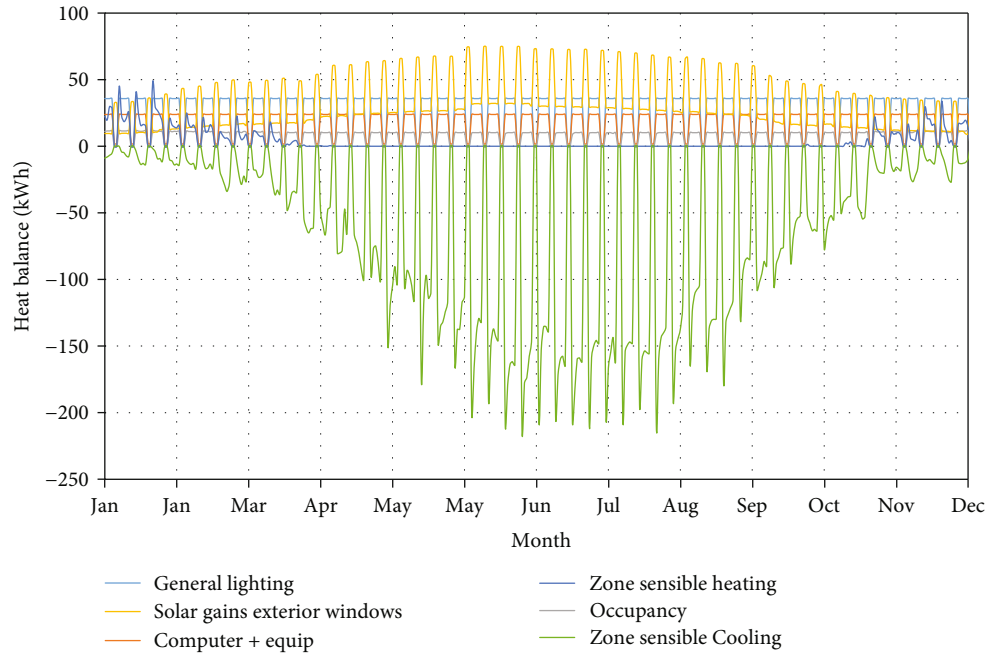

Figure 11: Daily consumed energy of the building within a year.

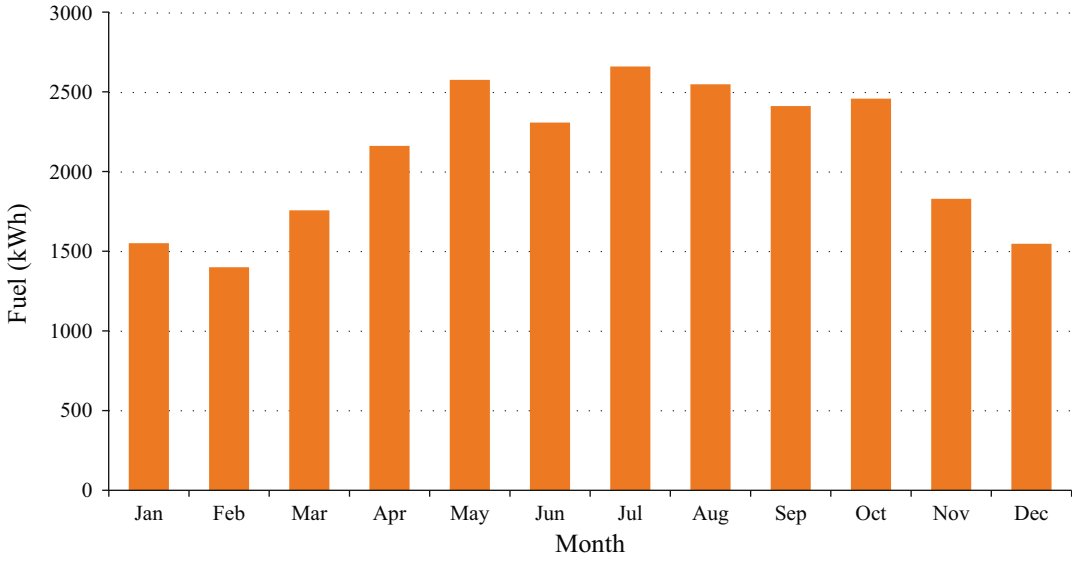

Figure 12: The total monthly consumed load of the building without consideration of energy production.

of electrical energy used for the activity of residents and all equipment except lighting, electrical energy consumed for lighting, electrical energy consumed for cooling, and electrical energy consumed for supplying hot water were 6459.8 kWh, 9335.8 kWh, 8860.5 kWh, and 584.5 kWh, respectively, although the annual rate of electricity generation was 29902.9 kWh. Finally, the annual rate of consumed electricity load of the building and the annual rate of electricity generation have been compared with each other by renewable energies in Figure 16. In fact, this figure represents an evidence that the total rate of annual energy generation of the building (derived from photovoltaic panels installed in the roof of the building and also wind turbine) was marginally higher than the annual energy consumption of the building, and consequently, the building has become net-zero energy from the perspective of energy consumption.

3.3. Thermal Comfort Analysis. Using the CFD analyses implemented in this study and by obtaining the variation of the temperature, velocity, and other parameters, the thermal predicted percentage of dissatisfied residents of the studied building has been obtained and is shown in Figures 17 and

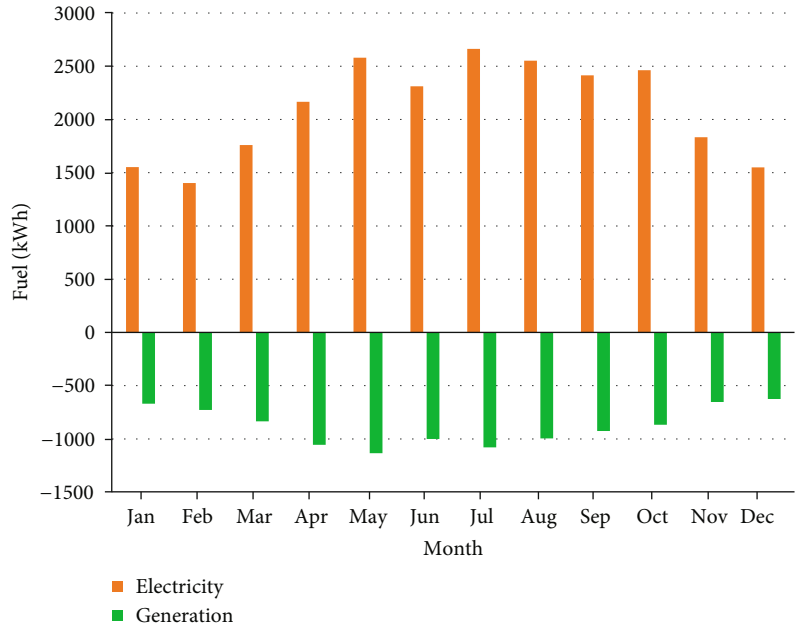

Figure 13: The total monthly consumed and produced load of the building with consideration of photovoltaic panel production.

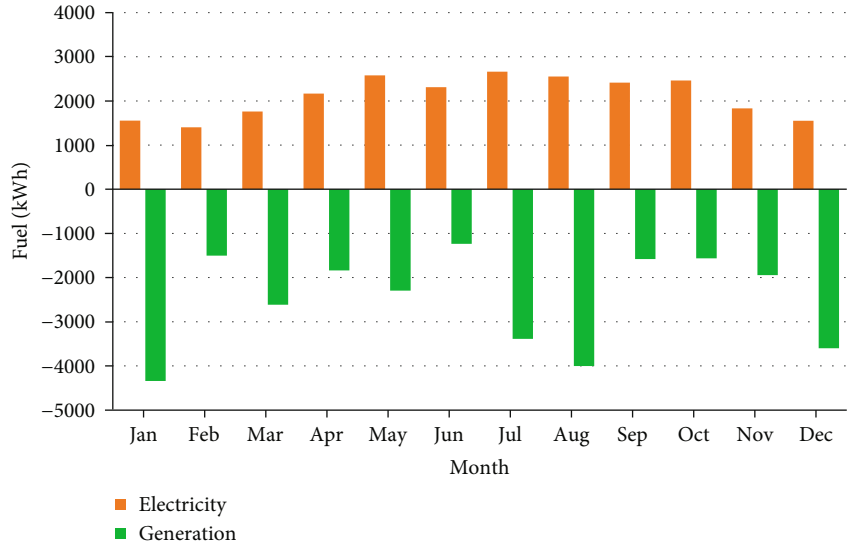

Figure 14: Total monthly produced and consumed loads of the building with consideration of photovoltaic panel and wind turbine production.

18 (side view and 3D view of building). As shown, the location of the highest thermal predicted percentage of dissatisfied residents of the studied building was around the windows, and the lowest amount was in areas far from sunlight. The reason for this is also justified by exposure to sunlight and also airflow infiltration near the windows.

A comparison of thermal comfort between the three models of Fanger, Pierce, and the University of Kansas over a one-year period has been presented in Figure 19. As can be seen, Fanger's model has more scattering throughout the year, while the proposed model of the University of Kansas has less scattering. It is also evident that Pierce's model reports the highest index of thermal comfort between March and November. In any case, the best thermal comfort of the studied building was in April and October according to the figure and all three models confirm this.

4. Conclusion

Current global approaches are based on unsustainable and nonrenewable energies. Nowadays, world energy supply is founded upon fossil fuels and atomic energy. These energy sources are not ever lasting and they are proven to create environmental problems. In less than three centuries after

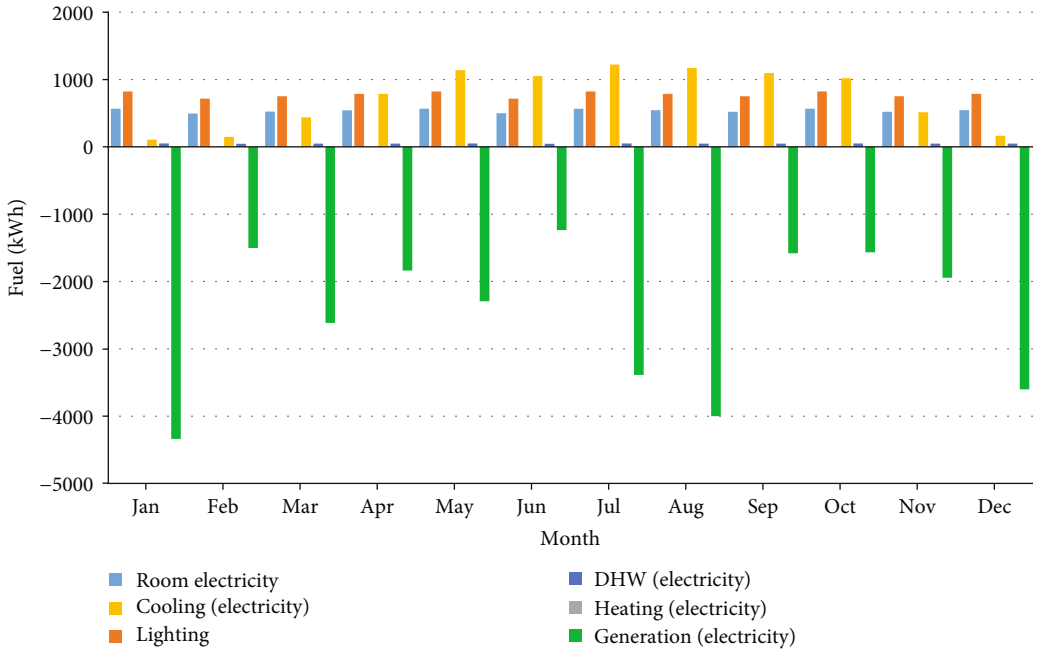

Figure 15: Monthly consumed and produced energies using renewable energies of the building within a year.

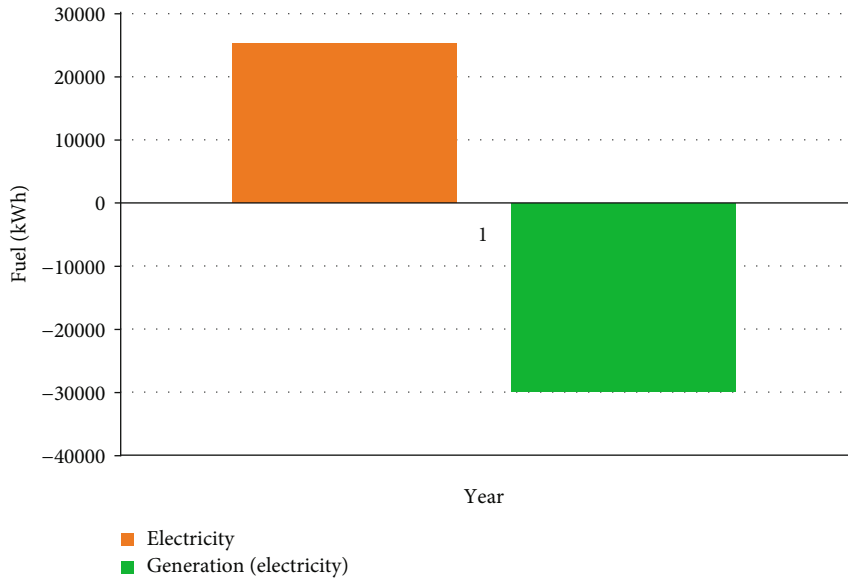

Figure 16: Total annual consumed and produced energies using renewable energies of the building.

the Industrial revolution, humankind have consumed almost half of the fossil fuels accumulated on the surface of the Earth and beneath it. Further, the power of atomic energy is at the mercy of limited uranium sources, and the risks of nuclear power plants are also undeniable. In addition, after fifty years of research, no site has been identified for long-time disposal of radioactive waste. Although some of fossil fuel sources may sustain longer than the predicted time, especially if new reservoirs are discovered, there still remains the main problem, i.e., "running out", indicating the biggest challenge for mankind. The energy used in the building sector is increasing on a daily basis because new buildings are built faster and in larger numbers than old buildings which are demolished. Electricity consumption in the commercial building sector doubled in the 1980-2000 interval, and it is expected to increase by another 50% by 2025, which fully reveals the necessity to shift to zero energy homes [2].

Advantages of net-zero energy buildings include

(i) Reduction of thermal fluctuations in these buildings, which results from adequate isolation and well provides the comfort conditions

(ii) Energy supply, even in the event of shut down in the global energy distribution network

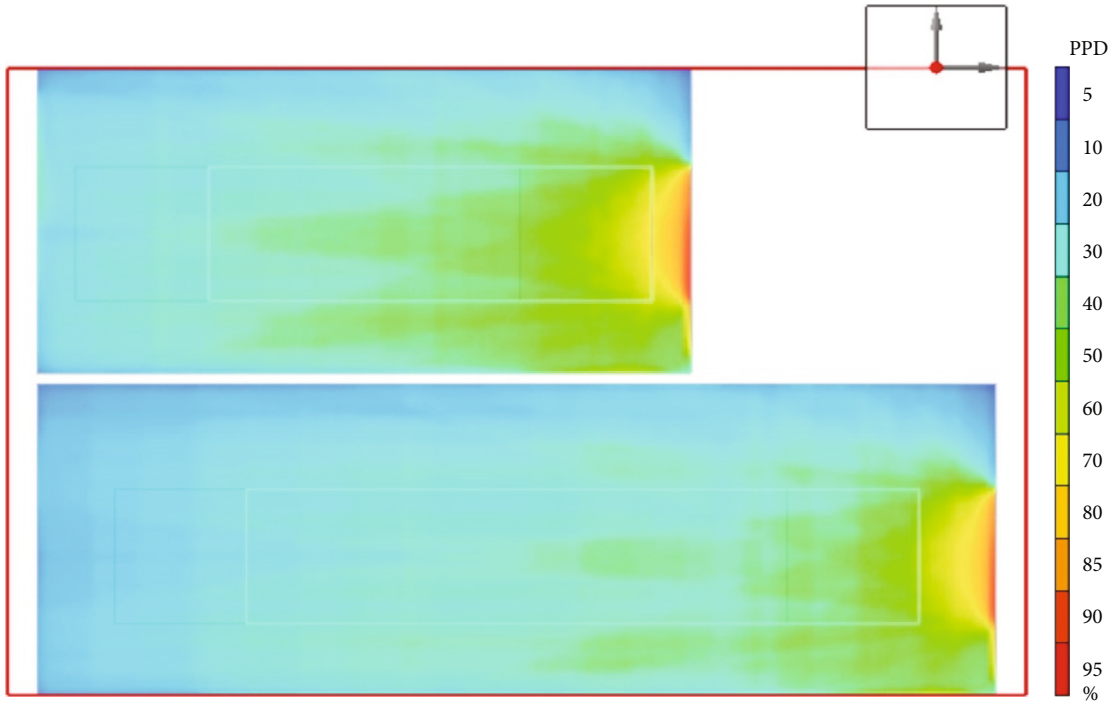

Figure 17: The thermal predicted percentage of dissatisfied residents of the studied building (side view).

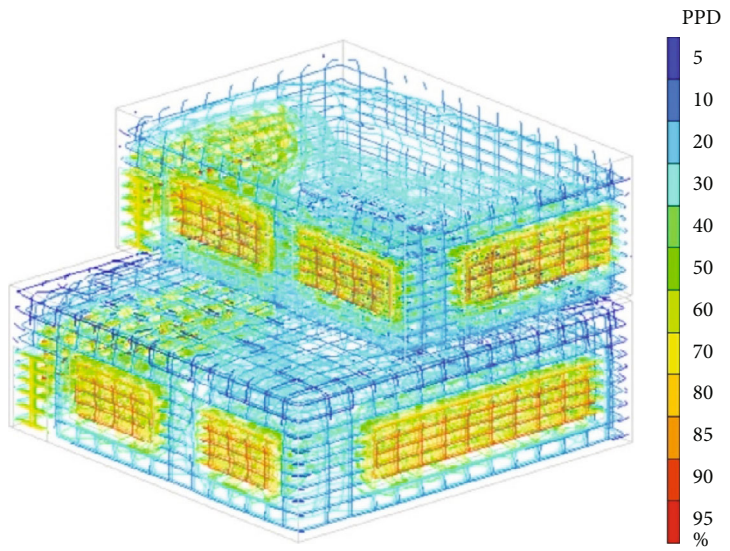

Figure 18: The thermal predicted percentage of dissatisfied residents of the studied building (3D view).

(iii) Protection against the ever increasing rise in energy prices

(iv) Reduction of greenhouse gases

(v) Savings in energy consumption

The findings of the present study illustrated that using photovoltaic panels alone is not able to create a net-zero energy building; rather, other types of renewable energy should be used along with the solar energy. Addition of wind turbines as a source of energy generation was analyzed in this study. It was observed that using wind turbines for electricity generation in cold seasons is an appropriate substitute for reduction of the electricity generated by photovoltaic panels in such seasons. Then, the best possible condition for the said building was provided through optimization of the two target parameters of reduction of the overall energy consumption of buildings, as well as a reduction of the number of hours of occupants' thermal dissatisfaction. Although almost 30% of energy consumption in warm months is for the lighting of office buildings, 45% of electricity is consumed to cool buildings. This is while around 50% of the energy consumed in

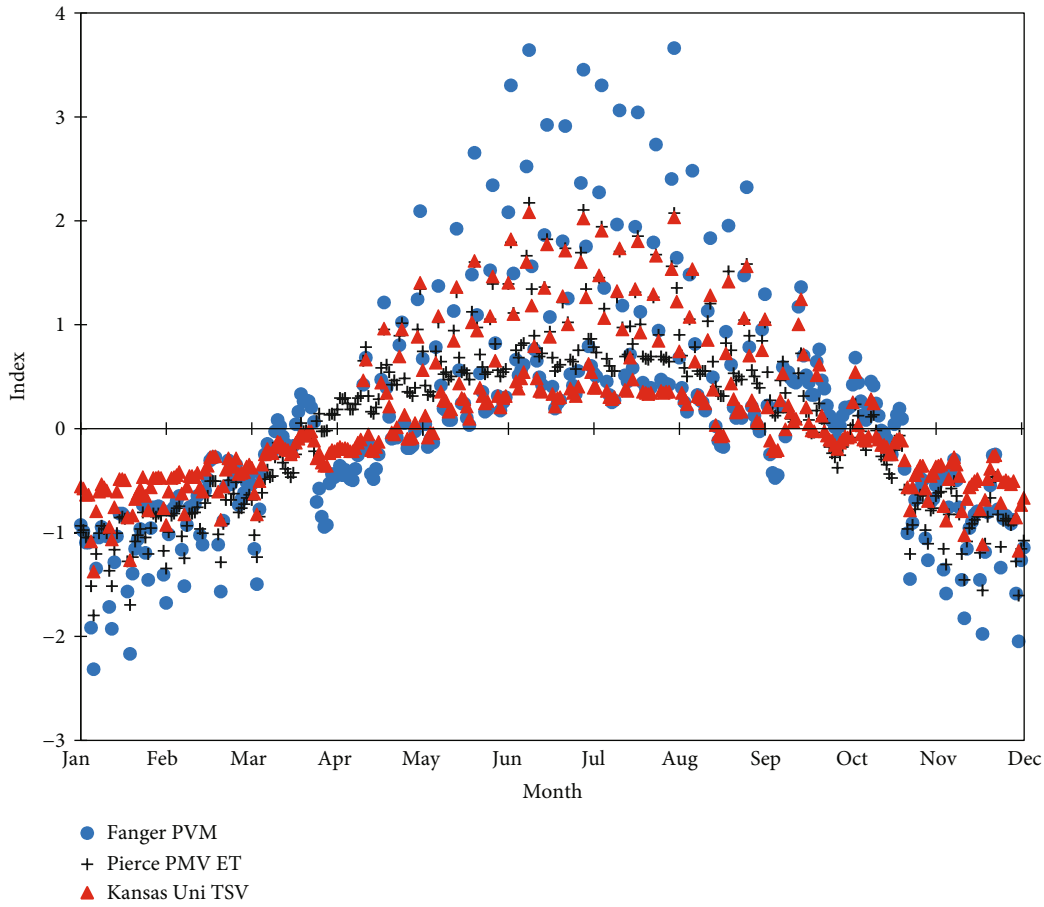

Figure 19: Comparison of thermal comfort in the studied building using three different methods.

cold months of the year is dedicated to lighting purposes. It was also observed that the amount of the energy generated in the month of January was four times higher than the amount generated in the month of June. Ultimately, the amount of the total annual net electricity energy dedicated to the global electricity network equals 4655 kWh, accounting for almost 18% of the total net electricity consumed in this building.

The findings of this study also illustrate that there is a good correspondence among the three thermal comfort models developed by Fanger, Pierce, and Kansas State University. Furthermore, April and October are the best months for experiencing thermal comfort in buildings, and clearly, occupants will undergo the greatest thermal comfort dissatisfaction in the warm months of the year. It was also observed that unlike the other two models, Fanger's model has the largest variance—particularly in warm months of the year—and reports the largest figures for the thermal comfort range as well.

Data Availability

The data used to support the findings of this study are included within the article.

Conflicts of Interest

The authors declare that there is no conflict of interest.

References

[1] N. Y. Jadhav, *Green and Smart Building - Advanced Technology Options*, Springer, Singapore, 2016.

[2] M. Kordjamshidi, "*House rating schemes*," Springer, Berlin Heidelberg, 2011.

[3] S. Cao, K. Klein, S. Herkel, and K. Sirén, "Approaches to enhance the energy performance of a zero-energy building integrated with a commercial-scale hydrogen fueled zero-energy vehicle under Finnish and German conditions," *Energy Conversion and Management*, vol. 142, pp. 153–175, 2017.

[4] P. Aryal and T. Leephakpreeda, "CFD analysis on thermal comfort and energy consumption effected by partitions in air-conditioned building," *Energy Procedia*, vol. 79, pp. 183–188, 2015.

[5] S. Zhang, Y. Cheng, Z. Fang, C. Huan, and Z. Lin, "Optimization of room air temperature in stratum-ventilated rooms for both thermal comfort and energy saving," *Applied Energy*, vol. 204, pp. 420–431, 2017.

[6] S. Lu, B. Pang, Y. Qi, and K. Fang, "Field study of thermal comfort in non-air-conditioned buildings in a tropical island climate," *Applied Ergonomics*, vol. 66, pp. 89–97, 2018.

[7] F. R. d'Ambrosio Alfano, E. Ianniello, and B. I. Palella, "PMV-PPD and acceptability in naturally ventilated schools," *Building and Environment*, vol. 67, pp. 129–137, 2013.

[8] Z. Xu, G. Hu, C. J. Spanos, and S. Schiavon, "PMV-based event-triggered mechanism for building energy management under uncertainties," *Energy and Buildings*, vol. 152, pp. 73–85, 2017.

[9] K. Fabbri, "Thermal comfort evaluation in kindergarten: PMV and PPD measurement through datalogger and questionnaire," *Building and Environment*, vol. 68, pp. 202–214, 2013.

[10] C. Hu and H. Li, "Deducing the classification rules for thermal comfort controls using optimal method," *Building and Environment*, vol. 98, pp. 107–120, 2016.

[11] R. Hwang and S. Shu, "Building envelope regulations on thermal comfort in glass facade buildings and energy-saving potential for PMV-based comfort control," *Building and Environment*, vol. 46, no. 4, pp. 824–834, 2011.

[12] D. H. Kang, P. H. Mo, D. H. Choi, S. Y. Song, M. S. Yeo, and K. W. Kim, "Effect of MRT variation on the energy consumption in a PMV-controlled office," *Building and Environment*, vol. 45, no. 9, pp. 1914–1922, 2010.

[13] J. T. Kim, J. H. Lim, S. H. Cho, and G. Y. Yun, "Development of the adaptive PMV model for improving prediction performances," *Energy and Buildings*, vol. 98, pp. 100–105, 2015.

[14] S. A. Nada, H. M. El-Batsh, H. F. Elattar, and N. M. Ali, "CFD investigation of airflow pattern, temperature distribution and thermal comfort of UFAD system for theater buildings applications," *Journal of Building Engineering*, vol. 6, pp. 274–300, 2016.

[15] J. A. Orosa and A. C. Oliveira, "A new thermal comfort approach comparing adaptive and PMV models," *Renewable Energy*, vol. 36, no. 3, pp. 951–956, 2011.

[16] A. Pourshaghaghy and M. Omidvari, "Examination of thermal comfort in a hospital using PMV-PPD model," *Applied Ergonomics*, vol. 43, no. 6, pp. 1089–1095, 2012.

[17] A. A. Volkov, A. V. Sedov, and P. D. Chelyshkov, "Modelling the thermal comfort of internal building spaces in social buildings," *Procedia Engineering*, vol. 91, pp. 362–367, 2014.

[18] M. F. Haniff, H. Selamat, N. Khamis, and A. J. Alimin, "Optimized scheduling for an air-conditioning system based on indoor thermal comfort using the multi-objective improved global particle swarm optimization," *Energy Efficiency*, vol. 12, no. 5, pp. 1183–1201, 2019.

[19] S. Wei, M. Li, W. Lin, and Y. Sun, "Parametric studies and evaluations of indoor thermal environment in wet season using a field survey and PMV-PPD method," *Energy and Buildings*, vol. 42, no. 6, pp. 799–806, 2010.

[20] S. Deng, A. Dalibard, M. Martin, Y. J. Dai, U. Eicker, and R. Z. Wang, "Energy supply concepts for zero energy residential buildings in humid and dry climate," *Energy Conversion and Management*, vol. 52, no. 6, pp. 2455–2460, 2011.

[21] W. Wu and H. M. Skye, "Net-zero nation: HVAC and PV systems for residential net-zero energy buildings across the United States," *Energy Conversion and Management*, vol. 177, pp. 605–628, 2018.

[22] E. P. B. D. Recast, "Directive 2010/31/EU of the European Parliament and of the Council of 19 May 2010 on the energy performance of buildings (recast)," *Official Journal of the European Union*, vol. 18, no. 6, 2010.

[23] F. Sarhaddi, S. Farahat, H. Ajam, A. Behzadmehr, and M. Mahdavi Adeli, "An improved thermal and electrical model for a solar photovoltaic thermal (PV/T) air collector," *Applied Energy*, vol. 87, no. 7, pp. 2328–2339, 2010.

[24] DesignBuilder, "Simulation hourly weather data," 2019, https://www.designbuilder.co.uk/content/view/144/223/.

[25] F. Ascione, N. Bianco, O. Böttcher, R. Kaltenbrunner, and G. P. Vanoli, "Net zero-energy buildings in Germany: design, model calibration and lessons learned from a case-study in Berlin," *Energy and Buildings*, vol. 133, pp. 688–710, 2016.

[26] T. Law, *The Future of Thermal Comfort in an Energy-Constrained World*, Springer International Publishing, Switzerland, 2013.

[27] P. O. Fanger, "Thermal comfort: analysis and applications in environmental engineering:," *Applied Ergonomics*, vol. 3, no. 3, p. 181, 1972.

[28] ISO EN 7730, *Ergonomics of the thermal environmentdanalytical determination and interpretation of thermal comfort using calculation of the PMV and PPD indices and local thermal comfort criteria*, International Organization for Standardization, 2005.

[29] K. Deb, A. Pratap, S. Agarwal, and T. Meyarivan, "A fast and elitist multiobjective genetic algorithm: NSGA-II," *IEEE Transactions on Evolutionary Computation*, vol. 6, no. 2, pp. 182–197, 2002.